ACS MATERIALS LETTERS

Cite This: ACS Materials Lett. 2019, 1, 613–619

www.acsmaterialslett.org

LETTER

Aggregation-Induced Delayed Fluorescence Luminogens with Accelerated Reverse Intersystem Crossing for High-Performance OLEDs

Jingwen Xu,[†,‡] Xiangyu Zhu,[†,‡] Jingjing Guo,[†] Jianzhong Fan,[⊥] Jiajie Zeng,[†] Shuming Chen,[§] Zujin Zhao,*[,†] and Ben Zhong Tang*[†,∥]

[†]State Key Laboratory of Luminescent Materials and Devices, Key Laboratory of Luminescence from Molecular Aggregates of Guangdong Province, South China University of Technology, Guangzhou 510640, China

[⊥]Shandong Province Key Laboratory of Medical Physics and Image Processing Technology, Institute of Materials and Clean Energy, School of Physics and Electronics, Shandong Normal University, Jinan 250014, China

[§]Department of Electrical and Electronic Engineering, Southern University of Science and Technology, Shenzhen, Guangdong 518055, China

[∥]Department of Chemistry, Hong Kong University of Science & Technology, Clear Water Bay, Kowloon, Hong Kong China

Supporting Information

ABSTRACT: **A fast reverse intersystem crossing (RISC) is of high importance for delayed fluorescence emitters in terms of increasing exciton utilization and suppressing efficiency roll-off. Herein, new robust luminogens comprised of carbonyl, phenoxazine, and chlorine-substituted carbazole derivatives are synthesized and characterized. They have distinct aggregation-induced delayed fluorescence (AIDF) features and exhibit high photoluminescence efficiencies and short delayed fluorescence lifetimes in neat films. The RISC is conspicuously accelerated because of their tiny singlet−triplet energy splitting and greatly enhanced spin−orbit coupling by heavy atom effect in neat films. They can function efficiently as light-emitting layers in nondoped OLEDs, providing excellent maximum electroluminescence (EL) efficiencies of 20.4−21.7%, and can also perform outstandingly in doped OLEDs in a wide doping concentration range (5−90 wt %), affording impressive EL efficiencies of up to 100.1 cd A^{-1}, 104.8 lm W^{-1}, and 29.1%, with small efficiency roll-off. These findings demonstrate the AIDF luminogens with fast RISC are promising candidates to fulfill various demands of production and application of OLEDs.**

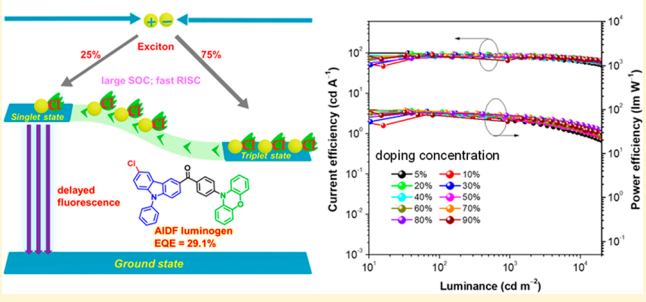

Delayed fluorescence is an important photophysical phenomenon, involving triplet to singlet spin conversion via reverse intersystem crossing (RISC) or triplet−triplet annihilation (TTA) processes. The occurrence of RISC generally requires a small singlet−triplet energy splitting (ΔE_{ST}) of the molecule, while TTA relies on collisional energy transfer between two triplet states (excitons). It is RISC that enables the current riveting purely organic thermally activated delayed fluorescence (TADF) materials to harvest electrogenerated triplet excitons for light emission to achieve exciting breakthrough of theoretically 100% exciton utilization for organic light-emitting diodes (OLEDs).[1−23] A fast RISC, corresponding to a short lifetime of delayed fluorescence ($\tau_{delayed}$), can effectively reduce triplet exciton concentration and thus suppress TTA at high voltages.[24−34] As a result, more triplet excitons can be harnessed to improve electroluminescence (EL) efficiencies, and the troublesome efficiency roll-off problem associated with TADF materials may be alleviated or even completely solved.

According to Fermi's Golden rule,[35−38] the rate constant of RISC (k_{RISC}) mainly depends on ΔE_{ST} and spin−orbit coupling (SOC), as expressed in formula 1

Received: September 6, 2019
Accepted: October 25, 2019
Published: October 25, 2019

DOI: 10.1021/acsmaterialslett.9b00369
ACS Materials Lett. 2019, 1, 613–619

$$k_{RISC} \propto \left| \left\langle \frac{\psi_1 | \hat{H}_{SO} | \psi_2}{\Delta E_{12}} \right\rangle \right|^2 \quad (1)$$

in which Ψ_1 and Ψ_2 represent the specific wave functions of initial and final states of RISC, respectively, $\hat{H}_{SO}$ is the operator for SOC, and ΔE_{12} is the energy difference between initial and final states. In consequence, RISC can be promoted by increasing SOC and decreasing ΔE_{ST}. Given a large enough SOC and a tiny ΔE_{ST} approaching zero, the RISC can be greatly accelerated. In general, the ΔE_{ST} can be lowered by separating highest occupied molecular orbital (HOMO) and lowest unoccupied molecular orbital (LUMO) via twisted connection of electron donor and acceptor. The formation of molecular aggregate is also conducive to diminishing ΔE_{ST} owing to energy splitting effect of excited states or hybridized local and charge transfer.[39−42] The SOC can be increased in the presence of atoms of high atomic number, namely, heavy atom effect, which is widely adopted in design of purely organic molecules with room temperature phosphorescence and TADF.[43−49] The heavy atom effect is usually categorized as internal and external heavy atom effects. In comparison to the internal heavy atom effect from the limited heavy atoms attached on central molecule, in the aggregated state, the external heavy atom effect exerted on the central molecule can be greatly amplified because of much more surrounding heavy atoms[50−53] and, thus, can play a more powerful role in enhancing SOC and perturbing spin statistics.

To create delayed fluorescence luminogens with a fast RISC, in this contribution, we design a series of new molecules bearing an electron-withdrawing carbonyl core and chlorine-substituted electron-donating groups (Figure 1A). The chlorine and

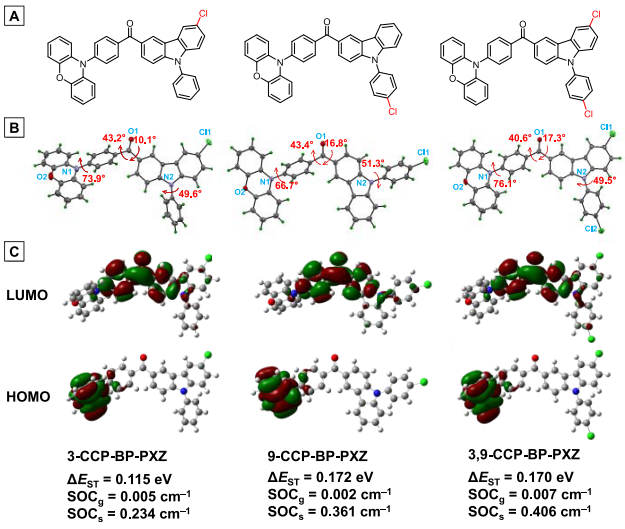

Figure 1. (A) Chemical and (B) crystal structures of 3-CCP-BP-PXZ, 9-CCP-BP-PXZ, and 3,9-CCP-BP-PXZ. (C) Calculated frontier orbital amplitude plots, ΔE_{ST} and SOC values; SOC_g and SOC_s are the SOC values computed in gas and solid phases, respectively.

carbonyl have been proved to be capable of increasing SOC.[54−56] The chlorine is selected also because of the stronger chlorine−carbon bond than bromine−carbon and iodine−carbon bonds, which ensures relatively higher chemical stability of the luminogens with chlorine. The obtained luminogens exhibit high photoluminescence (PL) quantum yield (Φ_{PL}) and short $\tau_{delayed}$ values in neat films. The RISC obviously speeds up in the aggregated state owing to the enhanced SOC. These merits enable the luminogens to function outstandingly in nondoped and doped OLEDs at varied doping concentrations (5−90 wt %), with impressive EL efficiencies and small efficiency roll-off.

The new luminogens 3-CCP-BP-PXZ, 9-CCP-BP-PXZ, and 3,9-CCP-BP-PXZ are easily prepared in high yields by Friedel−Crafts acylations of chlorine-substituted carbazole derivatives and 4-fluorobenzoyl chloride, followed by coupling with phenoxazine (PXZ) in the presence of *t*-BuOK (Scheme S1). The differential scanning calorimeter and thermogravimetric analysis reveal high glass-transition temperatures of 92, 81, and 111 °C and high decomposition temperatures of 359, 417, and 422 °C for 3-CCP-BP-PXZ, 9-CCP-BP-PXZ, and 3,9-CCP-BP-PXZ, respectively (Figure S1), verifying their good thermal and morphological stabilities. They also hold high electrochemical stability as uncovered by the reversible oxidation and reduction processes in cyclic voltammetry measurement. Their practical HOMO and LUMO energy levels in neat films are determined as around −5.0 and −2.7 eV, respectively (Figure S2).

Single crystals of the new luminogens are cultured in dichloromethane−methanol mixtures by slow solvent evaporation, and analyzed by X-ray crystallography. As illustrated in Figure 1B, all the luminogens adopt twisted conformations. Taking 3-CCP-BP-PXZ as an example, the phenyl ring at 9-position of carbazole shows a torsion angle of 49.6°, and the phenyl ring between PXZ and central carbonyl forms large torsion angles of 73.9° and 43.2° with each other. However, the carbazole is connected with carbonyl in a relatively planar manner with a small torsion angle of 10.1°. These conformational findings suggest that it is much easier for PXZ and carbonyl to achieve separation of HOMO and LUMO. The twisted conformation can also efficiently suppress strong $\pi-\pi$ interaction that may lead to emission quenching and exciton annihilation. Numerous weak intermolecular interactions, including C−H···π, C═O···H and C−Cl···H, as well as C−Cl···π interactions, are observed in crystals (Figure S3), which are helpful to rigidify molecular structures and reduce nonradiative energy loss. Moreover, the interactions of chlorine and carbonyl with neighboring aromatic moieties can induce efficient orbital couplings (e.g., $\pi-\sigma^*$ and $n-\pi^*$).[57−59] Consequently, the luminogen can feel additional heavy atom effect from many surrounding chlorine and carbonyl groups in the aggregated state, like external heavy atom effect, which is conductive to SOC enhancement.

The twisted geometry of the new luminogens can facilitate separation of HOMOs and LUMOs. Indeed, as disclosed by theoretical calculation, the HOMOs are mainly located on PXZ, while the LUMOs are distributed on carbonyl, adjacent phenyl and a part of carbazole (Figure 1C), which agrees well with their crystal structures. The good separation of HOMOs and LUMOs results in small theoretical ΔE_{ST} values of 0.115−0.172 eV and, thus, ensures the occurrence of rapid RISC. On the other side, the SOC values of these luminogens in gas phase are calculated to be 0.002−0.007 cm^{-1}, while the SOC values in solid phase significantly boost to 0.234−0.406 cm^{-1}, which is attributed to the enhanced heavy atom effect in the aggregated state as discussed above.[49−53] These SOC values are also apparently larger than that of the chlorine-free parent CP-BP-PXZ (0.084 cm^{-1}) in solid. The large SOC values can greatly accelerate RISC and eventually bring about efficient delayed fluorescence with short lifetimes.

DOI: 10.1021/acsmaterialslett.9b00369
ACS Materials Lett. 2019, 1, 613−619

3-CCP-BP-PXZ, 9-CCP-BP-PXZ, and 3,9-CCP-BP-PXZ exhibit strong absorption bands at 326−328 nm and weak charge transfer absorption bands at ∼405 nm in THF solutions (Figure 2A) and emit weak PL at 571−576 nm with low Φ_{PL} values of 2.7−3.0% (Table 1) in THF solutions. Transient PL decay spectra reveal quite short mean PL lifetimes of 3.9−11.7 ns, and the delayed components are tiny (Table S1). However, upon formation of aggregates by adding a large amount of water into THF solutions, their PL intensifies and gets blue-shifted to 538−540 nm (Figures 2C and S4). The restriction of intramolecular motions by physical constraint and weak intermolecular interactions in aggregate can block non-radiative decay channel and reduce reorganization energy of excited state, leading to enhanced and blue-shifted emission.[60,61] On the other hand, the PL lifetimes become longer and the delayed fluorescence character becomes distinct as the aggregate formation (Figures 2D and S5). The transient PL decay curves can be fitted by double exponential decay, corresponding to prompt and delayed fluorescence. For example, at a high water fraction of 99 vol %, the mean PL lifetime of 3-CCP-BP-PXZ reaches 149 ns, and the delayed component with a lifetime of 0.57 μs is observed (Table S1). In view of the weak PL without noticeable delayed fluorescence in solutions, these results unveil that the delayed fluorescence of the luminogens is induced by aggregate formation, namely, aggregation-induced delayed fluorescence (AIDF).[27−34,62−65]

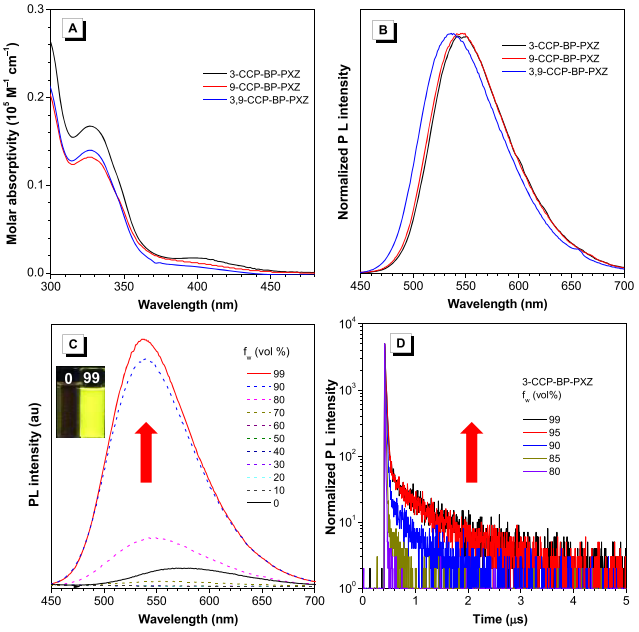

Figure 2. (A) Absorption spectra in THF (10^{-5} M) and (B) PL spectra in neat film of the new luminogens. (C) PL spectra and (D) PL decay curves of 3-CCP-BP-PXZ in THF/water mixtures with different water fractions (f_w) (10^{-5} M), measured under nitrogen atmosphere.

3-CCP-BP-PXZ, 9-CCP-BP-PXZ, and 3,9-CCP-BP-PXZ can luminesce strongly in neat films (Figure 2B), exhibiting PL peaks at 536−543 nm, high Φ_{PL} values of 70.4−73.0%, and mean PL lifetimes of 112−199 ns. The transient PL decay spectra disclose that 3-CCP-BP-PXZ and 9-CCP-BP-PXZ have relatively short $\tau_{delayed}$ values of 0.76 and 0.68 μs, corresponding to k_{RISC} values of 1.73×10^6 and 1.97×10^6 s^{-1}, respectively. 3,9-CCP-BP-PXZ, which carries more chlorine atoms, has an even shorter $\tau_{delayed}$ of 0.42 μs and a larger k_{RISC} of 3.10×10^6 s^{-1}. Combining the relatively longer $\tau_{delayed}$ (2.1 μs) and smaller k_{RISC} (0.63×10^6 s^{-1}) of the parent CP-BP-PXZ,[28] these data unquestionably demonstrate the RISC is indeed quickened as the introduction of chlorine atoms. More interestingly, temperature-dependent transient PL decay spectra show that the delayed fluorescence of these luminogens only change slightly as the temperature rises from 77 to 300 K (Figure S6), probably owing to that the large SOC values diminish the dependence of RISC on temperature, namely, the delayed fluorescence can occur efficiently even at low temperatures. The ΔE_{ST} values of the luminogens in neat films are as small as 0.016−0.019 eV, calculated from fluorescence and phosphorescence spectra at 77 K (Figure S7), smaller than that of CP-BP-PXZ (0.024 eV). So, the smaller ΔE_{ST} and enhanced SOC result in the faster RISC of the new luminogens. The eminent AIDF property and fast RISC enable the luminogens to function efficiently in both nondoped and doped OLEDs with high exciton utilization and small efficiency roll-off.

To study the EL performance of the new luminogens, nondoped OLEDs with a configuration of ITO/HATCN (5 nm)/TAPC (30 nm)/TCTA (5 nm)/emitter (20 nm)/TmPyPB (40 nm)/LiF (1 nm)Al are fabricated by vacuum deposition technique,[66] where the neat films of the luminogens function as light-emitting layers, HATCN serves as hole injection layer, TAPC and TmPyPB are used as hole- and electron-transporting layers, respectively, and TCTA works as electron-blocking layer. All the devices can be turned on at very low voltages of 2.6−2.8 V and illuminate strong yellow light at 537−541 nm, with peak luminance (L_{max}) of up to 88750 cd m^{-2} and stable EL spectra at varied voltages. These nondoped OLEDs exhibit outstanding EL efficiencies with maximum

Table 1. Photophysical Properties of the New AIDF Luminogens

	solution[a]				film[b]							
	λ_{abs} (nm)	λ_{em} (nm)	Φ_{PL}[c] (%)	$\langle\tau\rangle$[d] (ns)	λ_{em} (nm)	Φ_{PL}[c] (%)	$\langle\tau\rangle$[d] (ns)	τ_{prompt}[d] (ns)	$\tau_{delayed}$[d] (μs)	$R_{delayed}$[e] (%)	k_{RISC}[f] (10^6 s^{-1})	ΔE_{ST}[g] (eV)
3-CCP-BP-PXZ	327	575	3.0	11.7	541	73.0	199	22.2	0.76	24.0	1.73	0.016
9-CCP-BP-PXZ	328	571	2.8	10.3	543	70.4	188	22.2	0.68	25.2	1.97	0.018
3,9-CCP-BP-PXZ	326	576	2.7	3.9	536	72.6	112	21.1	0.42	22.7	3.10	0.019
CP-BP-PXZ[h]	330	582	2.2	11.8	530	58.0	512	23.5	2.10	24.0	0.63	0.024

[a]Measured in THF solution (10^{-5} M) at room temperature. [b]Vacuum-deposited on a quartz substrate. [c]Determined by a calibrated integrating sphere at room temperature under nitrogen atmosphere. [d]Mean fluorescence lifetimes ($\langle\tau\rangle$), and prompt (τ_{prompt}) and delayed ($\tau_{delayed}$) components evaluated at 300 K under nitrogen atmosphere. [e]Ratio of delayed ($R_{delayed}$) component evaluated at 300 K under nitrogen atmosphere. [f]The rate constant of RISC, calculated from the equations given in the Supporting Information. [g]Estimated from the high-energy onsets of fluorescence and phosphorescence spectra at 77 K. [h]The data are cited from ref 28.

DOI: 10.1021/acsmaterialslett.9b00369
ACS Materials Lett. 2019, 1, 613−619

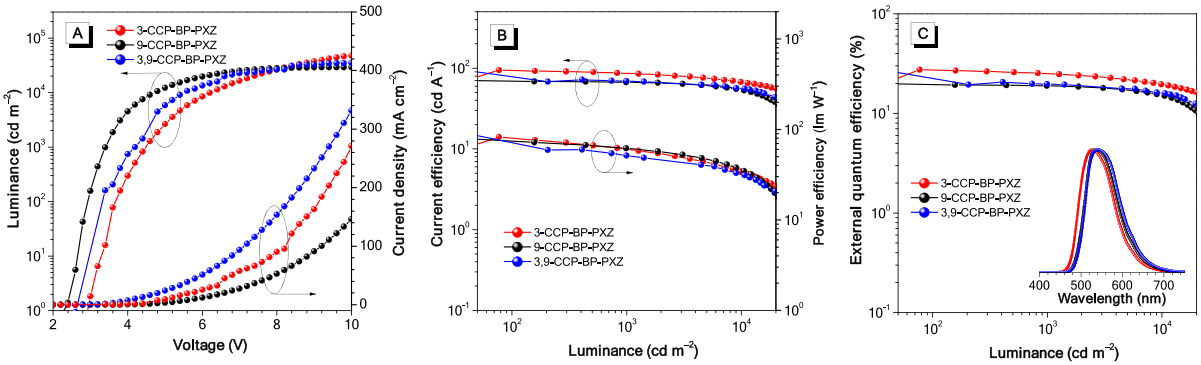

Figure 3. Plots of (A) luminance−voltage−current density, (B) current efficiency−luminance−power efficiency, and (C) external quantum efficiency−luminance of the nondoped OLEDs. Inset: EL spectra at 1000 cd m^{-2}. Device configuration: ITO/HATCN (5 nm)/TAPC (30 nm)/TCTA (5 nm)/emitter (20 nm)/TmPyPB (40 nm)/LiF (1 nm)/Al; emitter = 3-CCP-BP-PXZ, 9-CCP-BP-PXZ, or 3,9-CCP-BP-PXZ.

Table 2. EL Performances of the OLEDs Based on the New AIDF Luminogens[a]

		maximum values				values at 1000 cd m^{-2}					
	V_{on}(V)	η_C (cd A^{-1})	η_P (lm W^{-1})	η_{ext} (%)	L (cd m^{-2})	η_C (cd A^{-1})	η_P (lm W^{-1})	η_{ext} (%)	RO (%)	CIE (x,y)	λ_{EL} (nm)
nondoped OLEDs											
3-CCP-BP-PXZ	2.8	76.6	75.2	21.7	88750	69.8	52.2	19.8	8.7	(0.38, 0.58)	540
9-CCP-BP-PXZ	2.6	72.5	53.5	20.4	29510	68.5	43.1	19.4	4.9	(0.37, 0.59)	537
3,9-CCP-BP-PXZ	2.8	72.1	65.4	20.6	35580	69.0	51.6	19.7	4.4	(0.39, 0.58)	541
doped OLEDs											
5 wt % 3-CCP-BP-PXZ	3.0	100.1	104.8	29.1	76820	82.0	56.0	23.8	18.2	(0.32, 0.59)	523
10 wt % 3-CCP-BP-PXZ	3.0	94.7	82.6	27.5	76540	85.2	58.1	24.7	10.1	(0.33, 0.59)	528
20 wt % 3-CCP-BP-PXZ	2.8	96.2	94.4	27.7	93900	89.7	70.4	25.8	6.8	(0.34, 0.59)	530
30 wt % 3-CCP-BP-PXZ	2.8	93.1	91.4	27.1	99590	85.7	67.3	24.9	8.1	(0.36, 0.58)	530
40 wt % 3-CCP-BP-PXZ	2.8	88.6	99.3	24.7	105400	76.8	60.3	21.4	13.3	(0.35, 0.60)	533
50 wt % 3-CCP-BP-PXZ	2.6	85.7	86.7	23.9	107100	84.0	62.8	23.4	2.1	(0.37, 0.59)	538
60 wt % 3-CCP-BP-PXZ	2.6	85.3	89.3	24.1	102400	81.1	67.0	22.9	4.9	(0.36, 0.59)	534
70 wt % 3-CCP-BP-PXZ	2.6	87.2	97.8	24.6	111400	82.0	71.5	23.1	6.1	(0.36, 0.59)	532
80 wt % 3-CCP-BP-PXZ	2.6	84.0	101.4	23.8	108000	81.6	75.4	23.1	2.9	(0.38, 0.58)	539
90 wt % 3-CCP-BP-PXZ	2.6	85.0	95.3	23.8	104600	79.5	56.8	22.3	6.3	(0.39, 0.58)	539

[a]Abbreviations: V_{on}= turn-on voltage at 1 cd m^{-2}; η_C= current efficiency; η_P = power efficiency; η_{ext} = external quantum efficiency; L = luminance; RO = current efficiency roll-off from maximum value to that at 1000 cd m^{-2}; CIE = Commission Internationale de l'Eclairage coordinates. Device configuration: ITO/HATCN (5 nm)/TAPC (30 nm)/TCTA (5 nm)/emitter (20 nm)/TmPyPB (40 nm)/LiF (1 nm)Al; nondoped OLEDs emitter = 3-CCP-BP-PXZ, 9-CCP-BP-PXZ, and 3,9-CCP-BP-PXZ; doped OLEDs emitter = 3-CCP-BP-PXZ (x wt %): CBP; x = 5, 10, 20, 30, 40, 50, 60, 70, 80, and 90.

current ($\eta_{C,max}$), power ($\eta_{P,max}$), and external quantum ($\eta_{ext,max}$) efficiencies of 72.1−76.6 cd A^{-1}, 53.5−75.2 lm W^{-1}, and 20.4−21.7%, respectively (Figure 3). At 1000 cd m^{-2}, these devices still maintain good performances with η_C, η_P, and η_{ext} of 68.5−69.8 cd A^{-1}, 43.1−52.2 lm W^{-1}, and 19.4−19.8%, respectively. The corresponding efficiency roll-off is only 4.4−8.7% (Table 2). These data are clearly advanced in comparison with those of CP-BP-PXZ ($\eta_{C,max}$ = 59.1 cd A^{-1}; $\eta_{ext,max}$ = 18.4%)[28] and are among state-of-the-art results ever reported for nondoped OLEDs.[27−34]

To further evaluate the application potential of the new luminogens, doped OLEDs with the same device configurations are fabricated. The emitters are comprised of doped films of the luminogens in 4,4′-di(carbazol-9-yl)-1,1′-biphenyl (CBP) host with varied doping concentrations from 5 to 90 wt %. The obtained doped OLEDs also show excellent EL performances. As listed in Table 2, the doped OLEDs of 3-CCP-BP-PXZ show low turn-on voltages of 2.6−3.0 V and intense EL with large L_{max} values of 76540−111400 cd m^{-2}. The device at 5 wt % doping concentration radiates green EL at 523 nm and holds the best EL efficiencies, with a $\eta_{C,max}$ of 100.1 cd A^{-1}, a $\eta_{P,max}$ of 104.8 lm W^{-1}, and a $\eta_{ext,max}$ of 29.1%. Interestingly, as the increase of doping concentration, the EL efficiencies virtually only have small changes. For example, even at a high concentration of 80 wt %, the $\eta_{C,max}$, $\eta_{P,max}$, and $\eta_{ext,max}$ are still as high as 84.0 cd A^{-1}, 101.4 lm W^{-1}, and 23.8%, respectively. More importantly, efficiency roll-off of these doped devices are much smaller than those of most doped OLEDs based on TADF materials. For example, the efficiency roll-off of 80 wt % 3-CCP-BP-PXZ device only exhibits a minor efficiency roll-off 2.9% at 1000 cd m^{-2}. The doped OLEDs of 9-CCP-BP-PXZ and 3,9-CCP-BP-PXZ also exhibit concentration-insensitive feature, as evidenced by stable $\eta_{ext,max}$ values of 20.4−24.1% and 20.0−26.5%, respectively, in a wide doping concentration range of 5−90 wt % (Figures S8 and S9). The device of 9-CCP-BP-PXZ at 40 wt % doping concentration provides a $\eta_{C,max}$ of 81.3 cd A^{-1}, a $\eta_{P,max}$ of 85.1 lm W^{-1}, and a $\eta_{ext,max}$ of 24.1%, with a small efficiency roll-off of 4.9% at 1000 cd m^{-2} (Table S3). The 3,9-CCP-BP-PXZ device at 20 wt % doping concentration affords a $\eta_{C,max}$ of 92.1 cd A^{-1}, a $\eta_{P,max}$ of 90.4 lm W^{-1}, and a $\eta_{ext,max}$ of 26.5%, with a small

DOI: 10.1021/acsmaterialslett.9b00369
ACS Materials Lett. 2019, 1, 613−619

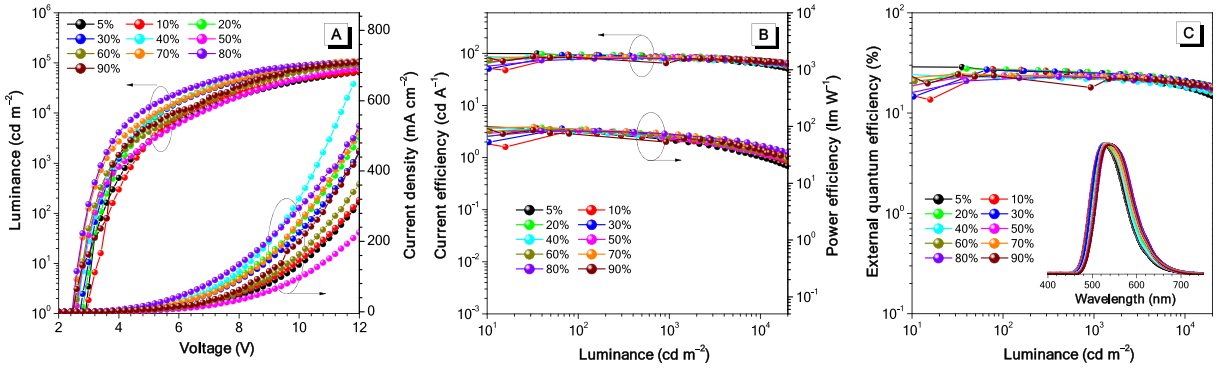

Figure 4. Plots of (A) luminance−voltage−current density, (B) current efficiency−luminance−power efficiency, and (C) external quantum efficiency−luminance of the doped OLEDs. Inset: EL spectra at 1000 cd m^{-2}. Device configuration: ITO/HATCN (5 nm)/TAPC (30 nm)/TCTA (5 nm)/3-CCP-BP-PXZ (*x* wt %): CBP (20 nm)/TmPyPB (40 nm)/LiF (1 nm)/Al; *x* = 5, 10, 20, 30, 40, 50, 60, 70, 80, or 90.

efficiency roll-off of 9.4% at 1000 cd m^{-2} (Table S4). These interesting results suggest that the short-range Dexter energy transfer has been successfully suppressed,[27−34,67,68] which enable the luminogens to perform efficiently at varied doping concentrations, without causing large performance variation and severe efficiency roll-off.

In summary, a series of new robust luminogens containing an electron-withdrawing carbonyl core and chlorine-substituted electron-donating groups are designed and synthesized. The new luminogens 3-CCP-BP-PXZ, 9-CCP-BP-PXZ, and 3,9-CCP-BP-PXZ have excellent thermal and electrochemical stabilities, and exhibit intriguing AIDF property, with higher Φ_{PL} and shorter $\tau_{delayed}$ values than those of chlorine-free CP-BP-PXZ. The tiny ΔE_{ST} and greatly enhanced SOC values in neat films, owing to strengthened heavy atom effect, significantly accelerate RISC and thus shorten $\tau_{delayed}$. The nondoped OLEDs of the luminogens exhibit remarkable EL performance, providing high $\eta_{C,max}$, $\eta_{P,max}$, and $\eta_{ext,max}$ of up to 76.6 cd A^{-1}, 75.2 lm W^{-1}, and 21.7%, respectively, with very small efficiency roll-off. The luminogens can also function robustly in doped OLEDs in a wide doping concentration range (5−90 wt %) with minor EL efficiency variation. Impressively high $\eta_{C,max}$, $\eta_{P,max}$, and $\eta_{ext,max}$ of 100.1 cd A^{-1}, 104.8 lm W^{-1}, and 29.1%, respectively, are attained in the doped OLEDs of 3-CCP-BP-PXZ. The eminent AIDF character, fast RISC and remarkable concentration-insensitive EL property demonstrate the new luminogens can be promising candidates to improve OLED production tolerance and operational stability.

■ ASSOCIATED CONTENT

Supporting Information

The Supporting Information is available free of charge on the ACS Publications website at DOI: 10.1021/acsmaterialslett.9b00369.

General information, synthesis and characterization, OLED fabrication and characterization, TGA and DSC curves, cyclic voltammograms, molecular packing in crystals, PL spectra in THF/water mixtures, transient PL decay spectra, fluorescence and phosphorescence spectra in neat films, photophysical data, character curves and key values of doped OLEDs of 9-CCP-BP-PXZ and 3,9-CCP-BP-PXZ, and NMR spectra (PDF)

Crystal data of 3-CCP-BP-PXZ (CIF)

Crystal data of 9-CCP-BP-PXZ (CIF)

Crystal data of 3,9-CCP-BP-PXZ (CIF)

■ AUTHOR INFORMATION

Corresponding Author

*E-mail: mszjzhao@scut.edu.cn.

ORCID

Zujin Zhao: 0000-0002-0618-6024

Ben Zhong Tang: 0000-0002-0293-964X

Author Contributions

‡J.X. and X.Z. contributed equally to this work.

Notes

The authors declare no competing financial interest.

■ ACKNOWLEDGMENTS

This work was financially supported by the National Natural Science Foundation of China (21788102), the Natural Science Foundation of Guangdong Province (2019B030301003), and the Science and Technology Program of Guangzhou (201804020027).

■ REFERENCES

(1) Uoyama, H.; Goushi, K.; Shizu, K.; Nomura, H.; Adachi, C. Highly Efficient Organic Light-Emitting Diodes from Delayed Fluorescence. *Nature* **2012**, *492*, 234−238.

(2) Zhang, Q.; Li, J.; Shizu, K.; Huang, S.; Hirata, S.; Miyazaki, H.; Adachi, C. Design of Efficient Thermally Activated Delayed Fluorescence Materials for Pure Blue Organic Light Emitting Diodes. *J. Am. Chem. Soc.* **2012**, *134*, 14706−14709.

(3) Hirata, S.; Sakai, Y.; Masui, K.; Tanaka, H.; Lee, S. Y.; Nomura, H.; Nakamura, N.; Yasumatsu, M.; Nakanotani, H.; Zhang, Q.; Shizu, K.; Miyazaki, H.; Adachi, C. Highly Efficient Blue Electroluminescence Based on Thermally Activated Delayed Fluorescence. *Nat. Mater.* **2015**, *14*, 330−336.

(4) Wu, T.-L.; Huang, M.-J.; Lin, C.-C.; Huang, P.-Y.; Chou, T.-Y.; Chen-Cheng, R.-W.; Lin, H.-W.; Liu, R.-S.; Cheng, C.-H. Diboron compound-based Organic Light-Emitting Diodes with High Efficiency and Reduced Efficiency Roll-Off. *Nat. Photonics* **2018**, *12*, 235−240.

(5) Ahn, D. H.; Kim, S. W.; Lee, H.; Ko, I. J.; Karthik, D.; Lee, J. Y.; Kwon, J. H. Highly Efficient Blue Thermally Activated Delayed Fluorescence Emitters Based on Symmetrical and Rigid Oxygen-Bridged Boron Acceptors. *Nat. Photonics* **2019**, *13*, 540−546.

(6) Tao, Y.; Yuan, K.; Chen, T.; Xu, P.; Li, H.; Chen, R.; Zheng, C.; Zhang, L.; Huang, W. Thermally Activated Delayed Fluorescence Materials Towards the Breakthrough of Organoelectronics. *Adv. Mater.* **2014**, *26*, 7931−7958.

(7) Cao, X.; Zhang, D.; Zhang, S.; Tao, Y.; Huang, W. CN-Containing Donor−Acceptor-Type Small-Molecule Materials for Thermally Activated Delayed Fluorescence OLEDs. *J. Mater. Chem. C* **2017**, *5*, 7699−7714.

DOI: 10.1021/acsmaterialslett.9b00369
ACS Materials Lett. 2019, 1, 613−619

(8) Rajamalli, P.; Senthilkumar, N.; Gandeepan, P.; Huang, P. Y.; Huang, M. J.; Ren-Wu, C. Z.; Yang, C. Y.; Chiu, M. J.; Chu, L. K.; Lin, H. W.; Cheng, C. H. A New Molecular Design Based on Thermally Activated Delayed Fluorescence for Highly Efficient Organic Light Emitting Diodes. *J. Am. Chem. Soc.* **2016**, *138*, 628−634.
(9) Rajamalli, P.; Senthilkumar, N.; Huang, P. Y.; Ren-Wu, C. C.; Lin, H. W.; Cheng, C. H. New Molecular Design Concurrently Providing Superior Pure Blue, Thermally Activated Delayed Fluorescence and Optical Out-Coupling Efficiencies. *J. Am. Chem. Soc.* **2017**, *139*, 10948−10951.
(10) Xie, G.; Luo, J.; Huang, M.; Chen, T.; Wu, K.; Gong, S.; Yang, C. Inheriting the Characteristics of TADF Small Molecule by Side-Chain Engineering Strategy to Enable Bluish-Green Polymers with High PLQYs up to 74% and External Quantum Efficiency over 16% in Light-Emitting Diodes. *Adv. Mater.* **2017**, *29*, 1604223.
(11) Li, C.; Duan, C.; Han, C.; Xu, H. Secondary Acceptor Optimization for Full-Exciton Radiation: Toward Sky-Blue Thermally Activated Delayed Fluorescence Diodes with External Quantum Efficiency of approximately 30. *Adv. Mater.* **2018**, *30*, 1804228.
(12) Tsai, K. W.; Hung, M. K.; Mao, Y. H.; Chen, S. A. Solution-Processed Thermally Activated Delayed Fluorescent OLED with High EQE as 31% Using High Triplet Energy Crosslinkable Hole Transport Materials. *Adv. Funct. Mater.* **2019**, *29*, 1901025.
(13) Shao, S.; Hu, J.; Wang, X.; Wang, L.; Jing, X.; Wang, F. Blue Thermally Activated Delayed Fluorescence Polymers with Non-conjugated Backbone and Through-Space Charge Transfer Effect. *J. Am. Chem. Soc.* **2017**, *139*, 17739−17742.
(14) Wex, B.; Kaafarani, B. R. Perspective on Carbazole-Based Organic Compounds as Emitters and Hosts in TADF Applications. *J. Mater. Chem. C* **2017**, *5*, 8622−8653.
(15) Godumala, M.; Choi, S.; Cho, M. J.; Choi, D. H. Thermally Activated Delayed Fluorescence Blue Dopants and Hosts: From the Design Strategy to Organic Light-Emitting Diode Applications. *J. Mater. Chem. C* **2016**, *4*, 11355−11381.
(16) Yang, Z.; Mao, Z.; Xie, Z.; Zhang, Y.; Liu, S.; Zhao, J.; Xu, J.; Chi, Z.; Aldred, M. P. Recent Advances in Organic Thermally Activated Delayed Fluorescence Materials. *Chem. Soc. Rev.* **2017**, *46*, 915−1016.
(17) Wong, M. Y.; Zysman-Colman, E. Purely Organic Thermally Activated Delayed Fluorescence Materials for Organic Light-Emitting Diodes. *Adv. Mater.* **2017**, *29*, 1605444.
(18) Zhang, D.; Song, X.; Cai, M.; Kaji, H.; Duan, L. Versatile Indolocarbazole-Isomer Derivatives as Highly Emissive Emitters and Ideal Hosts for Thermally Activated Delayed Fluorescent OLEDs with Alleviated Efficiency Roll-Off. *Adv. Mater.* **2018**, *30*, 1705406.
(19) Dias, F. B.; Santos, J.; Graves, D. R.; Data, P.; Nobuyasu, R. S.; Fox, M. A.; Batsanov, A. S.; Palmeira, T.; Berberan-Santos, M. N.; Bryce, M. R.; Monkman, A. P. The Role of Local Triplet Excited States and D-A Relative Orientation in Thermally Activated Delayed Fluorescence: Photophysics and Devices. *Adv. Sci.* **2016**, *3*, 1600080.
(20) Dos Santos, P. L.; Ward, J. S.; Bryce, M. R.; Monkman, A. P. Using Guest-Host Interactions to Optimize the Efficiency of TADF OLEDs. *J. Phys. Chem. Lett.* **2016**, *7*, 3341−3346.
(21) Seo, J.-A.; Im, Y.; Han, S. H.; Lee, C. W.; Lee, J. Y. Unconventional Molecular Design Approach of High-Efficiency Deep Blue Thermally Activated Delayed Fluorescent Emitters Using Indolocarbazole as an Acceptor. *ACS Appl. Mater. Interfaces* **2017**, *9*, 37864−37872.
(22) Li, C.; Duan, R.; Liang, B.; Han, G.; Wang, S.; Ye, K.; Liu, Y.; Yi, Y.; Wang, Y. Deep-Red to Near-Infrared Thermally Activated Delayed Fluorescence in Organic Solid Films and Electroluminescent Devices. *Angew. Chem., Int. Ed.* **2017**, *56*, 11525−11529.
(23) Yuan, Y.; Hu, Y.; Zhang, Y.-X.; Lin, J.-D.; Wang, Y.-K.; Jiang, Z.-Q.; Liao, L.-S.; Lee, S.-T. Over 10% EQE Near-Infrared Electroluminescence Based on a Thermally Activated Delayed Fluorescence Emitter. *Adv. Funct. Mater.* **2017**, *27*, 1700986.
(24) Chen, Z.; Wu, Z.; Ni, F.; Zhong, C.; Zeng, W.; Wei, D.; An, K.; Ma, D.; Yang, C. Emitters with a Pyridine-3,5-dicarbonitrile Core and Short Delayed Fluorescence Lifetimes of About 1.5 μs: Orange-red TADF-Based OLEDs with Very Slow Efficiency Roll-Offs at High Luminance. *J. Mater. Chem. C* **2018**, *6*, 6543−6548.
(25) Wang, H.; Meng, L.; Shen, X.; Wei, X.; Zheng, X.; Lv, X.; Yi, Y.; Wang, Y.; Wang, P. Highly Efficient Orange and Red Phosphorescent Organic Light-Emitting Diodes with Low Roll-Off of Efficiency Using a Novel Thermally Activated Delayed Fluorescence Material as Host. *Adv. Mater.* **2015**, *27*, 4041−4047.
(26) Schmidbauer, S.; Hohenleutner, A.; König, B. Chemical Degradation in Organic Light-Emitting Devices: Mechanisms and Implications for the Design of New Materials. *Adv. Mater.* **2013**, *25*, 2114−2129.
(27) Liu, H.; Zeng, J.; Guo, J.; Nie, H.; Zhao, Z.; Tang, B. Z. High-Performance Non-doped OLEDs with Nearly 100% Exciton Use and Negligible Efficiency Roll-Off. *Angew. Chem., Int. Ed.* **2018**, *57*, 9290−9294.
(28) Huang, J.; Nie, H.; Zeng, J.; Zhuang, Z.; Gan, S.; Cai, Y.; Guo, J.; Zhao, Z.; Tang, B. Z.; et al. Highly Efficient Nondoped OLEDs with Negligible Efficiency Roll-Off Fabricated from Aggregation-Induced Delayed Fluorescence Luminogens. *Angew. Chem., Int. Ed.* **2017**, *56*, 12971−12976.
(29) Guo, J.; Li, X.-L.; Nie, H.; Luo, W.; Gan, S.; Hu, S.; Hu, R.; Qin, A.; Zhao, Z.; Su, S.-J.; Tang, B. Z. Achieving High-Performance Nondoped OLEDs with Extremely Small Efficiency Roll-Off by Combining Aggregation-Induced Emission and Thermally Activated Delayed Fluorescence. *Adv. Funct. Mater.* **2017**, *27*, 1606458.
(30) Guo, J.; Li, X.-L.; Nie, H.; Luo, W.; Hu, R.; Qin, A.; Zhao, Z.; Su, S.-J.; Tang, B. Z. Robust Luminescent Materials with Prominent Aggregation-Induced Emission and Thermally Activated Delayed Fluorescence for High-Performance Organic Light-Emitting Diodes. *Chem. Mater.* **2017**, *29*, 3623−3631.
(31) Huang, J.; Xu, Z.; Cai, Z.; Guo, J.; Guo, J.; Shen, P.; Wang, Z.; Zhao, Z.; Ma, D.; Tang, B. Z. Robust Luminescent Small Molecules with Aggregation-Induced Delayed Fluorescence for Efficient Solution-Processed OLEDs. *J. Mater. Chem. C* **2019**, *7*, 330−339.
(32) Zhang, P.; Zeng, J.; Guo, J.; Zhen, S.; Xiao, B.; Wang, Z.; Zhao, Z.; Tang, B. Z. New Aggregation-Induced Delayed Fluorescence Luminogens With Through-Space Charge Transfer for Efficient Non-doped OLEDs. *Front. Chem.* **2019**, *7*, 199.
(33) Chen, X.; Yang, Z.; Xie, Z.; Zhao, J.; Yang, Z.; Zhang, Y.; Aldred, M. P.; Chi, Z. An Efficient Yellow Thermally Activated Delayed Fluorescence Emitter with Universal Applications in Both Doped and Non-doped Organic Light-Emitting Diodes. *Mater. Chem. Front.* **2018**, *2*, 1017−1023.
(34) Xiang, S.; Huang, Z.; Sun, S.; Lv, X.; Fan, L.; Ye, S.; Chen, H.; Guo, R.; Wang, L. Highly Efficient Non-doped OLEDs Using Aggregation-Induced Delayed Fluorescence Materials Based on 10-Phenyl-10H-phenothiazine 5,5-dioxide derivatives. *J. Mater. Chem. C* **2018**, *6*, 11436−11443.
(35) Szabo, A.; Ostlund, N. S. *Modern Quantum Chemistry: Introduction to Advanced Electronic Structure Theory*; McGraw-Hill, 1989.
(36) Samanta, P. K.; Kim, D.; Coropceanu, V.; Brédas, J.-L. Up-Conversion Intersystem Crossing Rates in Organic Emitters for Thermally Activated Delayed Fluorescence: Impact of the Nature of Singlet vs Triplet Excited States. *J. Am. Chem. Soc.* **2017**, *139*, 4042−4051.
(37) Gibson, J.; Monkman, A. P.; Penfold, T. J. The Importance of Vibronic Coupling for Efficient Reverse Intersystem Crossing in Thermally Activated Delayed Fluorescence Molecules. *ChemPhysChem* **2016**, *17*, 2956−2961.
(38) Chen, X.-K.; Kim, D.; Brédas, J.-L. Thermally Activated Delayed Fluorescence (TADF) Path toward Efficient Electroluminescence in Purely Organic Materials: Molecular Level Insight. *Acc. Chem. Res.* **2018**, *51*, 2215−2224.
(39) Yang, L.; Wang, X.; Zhang, G.; Chen, X.; Zhang, G.; Jiang, J. Aggregation-Induced Intersystem Crossing: A Novel Strategy for efficient Molecular Phosphorescence. *Nanoscale* **2016**, *8*, 17422−17426.

DOI: 10.1021/acsmaterialslett.9b00369
ACS Materials Lett. 2019, 1, 613−619

(40) Fan, J.; Zhang, Y.; Zhou, Y.; Lin, L.; Wang, C. K. Excited state Properties of a Thermally Activated Delayed Fluorescence Molecule in Solid Phase Studied by Quantum Mechanics/Molecular Mechanics Method. *J. Phys. Chem. C* **2018**, *122*, 2358−2366.
(41) Fan, J.; Cai, L.; Lin, L.; Wang, C. K. Excited State Dynamics for Hybridized Local and Charge Transfer State Fluorescent Emitters with Aggregation-Induced Emission in the Solid Phase: a QM/MM Study. *Phys. Chem. Chem. Phys.* **2017**, *19*, 29872−29879.
(42) Wang, C.; Zhang, Q. Understanding Solid-State Solvation-Enhanced Thermally Activated Delayed Fluorescence Using a Descriptor-Tuned Screened Range-Separated Functional. *J. Phys. Chem. C* **2019**, *123*, 4407−4416.
(43) Li, Q.; Li, Z. The Strong Light-Emission Materials in the Aggregated State: What Happens from a Single Molecule to the Collective Group. *Adv. Sci.* **2017**, *4*, 1600484.
(44) Shi, H.; Song, L.; Ma, H.; Sun, C.; Huang, K.; Lv, A.; Ye, W.; Wang, H.; Cai, S.; Yao, W.; Zhang, Y.; Zheng, R.; An, Z.; Huang, W. Highly Efficient Ultralong Organic Phosphorescence through Intramolecular-Space Heavy-Atom Effect. *J. Phys. Chem. Lett.* **2019**, *10*, 595−600.
(45) Chen, H.; Yao, X.; Ma, X.; Tian, H. Amorphous, Efficient, Room-Temperature Phosphorescent Metal-Free Polymers and Their Applications as Encryption Ink. *Adv. Opt. Mater.* **2016**, *4*, 1397−1401.
(46) Gan, S.; Hu, S.; Li, X.-L.; Zeng, J.; Zhang, D.; Huang, T.; Luo, W.; Zhao, Z.; Duan, L.; Su, S.-J.; Tang, B. Z. Heavy Atom Effect of Bromine Significantly Enhances Exciton Utilization of Delayed Fluorescence Luminogens. *ACS Appl. Mater. Interfaces* **2018**, *10*, 17327−17334.
(47) Xiang, Y.; Zhao, Y.; Xu, N.; Gong, S.; Ni, F.; Wu, K.; Luo, J.; Xie, G.; Lu, Z.-H.; Yang, C. Halogen-Induced Internal Heavy-Atom Effect Shortening the Emissive Lifetime and Improving the Fluorescence Efficiency of Thermally Activated Delayed Fluorescence Emitters. *J. Mater. Chem. C* **2017**, *5*, 12204−12210.
(48) Kretzschmar, A.; Patze, C.; Schwaebel, S. T.; Bunz, U. H. F. Development of Thermally Activated Delayed Fluorescence Materials with Shortened Emissive Lifetimes. *J. Org. Chem.* **2015**, *80*, 9126−9131.
(49) Ward, J. S.; Nobuyasu, R. S.; Fox, M. A.; Batsanov, A. S.; Santos, J.; Dias, F. B.; Bryce, M. R. Bond Rotations and Heteroatom Effects in Donor-Acceptor-Donor Molecules: Implications for Thermally Activated Delayed Fluorescence and Room Temperature Phosphorescence. *J. Org. Chem.* **2018**, *83*, 14431−14442.
(50) Einzinger, M.; Zhu, T.; de Silva, P.; Belger, C.; Swager, T. M.; Van Voorhis, T.; Baldo, M. A. Shorter Exciton Lifetimes via an External Heavy-Atom Effect: Alleviating the Effects of Bimolecular Processes in Organic Light-Emitting Diodes. *Adv. Mater.* **2017**, *29*, 1701987.
(51) Zhang, W.; Jin, J.; Huang, Z.; Zhuang, S.; Wang, L. A New Way towards High-Efficiency Thermally Activated Delayed Fluorescence Devices via External Heavy-Atom Effect. *Sci. Rep.* **2016**, *6*, 30178.
(52) Zhang, D.; Duan, L.; Zhang, Y.; Cai, M.; Zhang, D.; Qiu, Y. Highly Efficient Hybrid Warm White Organic Light-Emitting Diodes Using a Blue Thermally Activated Delayed Fluorescence Emitter: Exploiting the External Heavy-Atom Effect. *Light: Sci. Appl.* **2015**, *4*, No. e232.
(53) Wang, J.; Wang, C.; Gong, Y.; Liao, Q.; Han, M.; Jiang, T.; Dang, Q.; Li, Y.; Li, Q.; Li, Z. Bromine-Substituted Fluorene: Molecular Structure, Br−Br Interactions, Room-Temperature Phosphorescence, and Tricolor Triboluminescence. *Angew. Chem., Int. Ed.* **2018**, *57*, 16821−16826.
(54) He, Z.; Gao, H.; Zhang, S.; Zheng, S.; Wang, Y.; Zhao, Z.; Ding, D.; Yang, B.; Zhang, Y.; Yuan, W. Z. Achieving Persistent, Efficient, and Robust Room-Temperature Phosphorescence from Pure Organics for Versatile Applications. *Adv. Mater.* **2019**, *31*, 1807222.
(55) He, Z.; Zhao, W.; Lam, J. W. Y.; Peng, Q.; Ma, H.; Liang, G.; Shuai, Z.; Tang, B. Z. White Light Emission from a Single Organic Molecule with Dual Phosphorescence at Room Temperature. *Nat. Commun.* **2017**, *8*, 416.
(56) Xie, Y.; Ge, Y.; Peng, Q.; Li, C.; Li, Q.; Li, Z. How the Molecular Packing Affects the Room Temperature Phosphorescence in Pure Organic Compounds: Ingenious Molecular Design, Detailed Crystal Analysis, and Rational Theoretical Calculations. *Adv. Mater.* **2017**, *29*, 1606829.
(57) Sun, X.; Zhang, B.; Li, X.; Trindle, C. O.; Zhang, G. External Heavy-Atom Effect via Orbital Interactions Revealed by Single-Crystal X-Ray Diffraction. *J. Phys. Chem. A* **2016**, *120*, 5791−5797.
(58) Mu, Y.; Yang, Z.; Chen, J.; Yang, Z.; Li, W.; Tan, X.; Mao, Z.; Yu, T.; Zhao, J.; Zheng, S.; Liu, S.; Zhang, Y.; Chi, Z.; Xu, J.; Aldred, M. P. Mechano-Induced Persistent Room-Temperature Phosphorescence from Purely Organic Molecules. *Chem. Sci.* **2018**, *9*, 3782−3787.
(59) Zhao, W.; He, Z.; Lam, J. W.Y.; Peng, Q.; Ma, H.; Shuai, Z.; Bai, G.; Hao, J.; Tang, B. Z. Rational Molecular Design for Achieving Persistent and Efficient Pure Organic Room-Temperature Phosphorescence. *Chem.* **2016**, *1*, 592−602.
(60) Mei, J.; Leung, N. L.; Kwok, R. T.; Lam, J. W.; Tang, B. Z. Aggregation-Induced Emission: Together We Shine, United We Soar! *Chem. Rev.* **2015**, *115*, 11718−11940.
(61) Luo, W.; Nie, H.; He, B.; Zhao, Z.; Peng, Q.; Tang, B. Z. Spectroscopic and Theoretical Characterization of Through-Space Conjugation of Foldamers with a Tetraphenylethene Hinge. *Chem. - Eur. J.* **2017**, *23*, 18041−18048.
(62) Guo, J.; Fan, J.; Lin, L.; Zeng, J.; Liu, H.; Wang, C. K.; Zhao, Z.; Tang, B. Z. Mechanical Insights into Aggregation-Induced Delayed Fluorescence Materials with Anti-Kasha Behavior. *Adv. Sci.* **2019**, *6*, 1801629.
(63) Guo, J.; Zhao, Z.; Tang, B. Z. Purely Organic Materials with Aggregation-Induced Delayed Fluorescence for Efficient Nondoped OLEDs. *Adv. Opt. Mater.* **2018**, *6*, 1800264.
(64) Liu, H.; Guo, J.; Zhao, Z.; Tang, B. Z. Aggregation-Induced Delayed Fluorescence. *ChemPhotoChem.* **2019**, *3*, 993−999.
(65) Furue, R.; Nishimoto, T.; Park, I. S.; Lee, J.; Yasuda, T. Aggregation-Induced Delayed Fluorescence Based on Donor/Acceptor-Tethered Janus Carborane Triads: Unique Photophysical Properties of Nondoped OLEDs. *Angew. Chem., Int. Ed.* **2016**, *55*, 7171−7175.
(66) ITO = indium tin oxide; HATCN = hexaazatriphenylenehexacabonitrile; TAPC = 1,1′-bis(di-4-tolylaminophenyl) cyclohexane; TmPyPB = 1,3,5-tri(m-pyrid-3-yl-phenyl)benzene; TCTA = tris(4-carbazoyl-9-ylphenyl)amine.
(67) Lee, J.; Aizawa, N.; Numata, M.; Adachi, C.; Yasuda, T. Versatile Molecular Functionalization for Inhibiting Concentration Quenching of Thermally Activated Delayed Fluorescence. *Adv. Mater.* **2017**, *29*, 1604856.
(68) Lee, J.; Aizawa, N.; Yasuda, T. Isobenzofuranone- and Chromone-Based Blue Delayed Fluorescence Emitters with Low Efficiency Roll-Off in Organic Light-Emitting Diodes. *Chem. Mater.* **2017**, *29*, 8012−8020.

DOI: 10.1021/acsmaterialslett.9b00369
ACS Materials Lett. 2019, 1, 613−619